20. Tanaka K, Uemoto S, Tokunaga Y et al (1993) Surgical techniques and innovations in living related liver transplantation. Ann Surg 217:82–91
21. Kasahara M, Ueda M, Haga H et al (2005) Living-donor liver transplantation for hepatoblastoma. Am J Transplant 5:2229–2235
22. Nishimura S, Sato T, Fujita N et al (2002) High-dose chemotherapy in children with metastatic hepatoblastoma. Pediatr Int 44:300–305
23. Yoshinari M, Imaizumi M, Hayashi Y et al (1998) Peripheral blood stem cell transplantation for hepatoblastoma with microscopical residue: a therapeutic approach for incompletely resected tumor. Tohoku J Exp Med 184:247–254
24. Kitahara S, Makuuchi M, Ishizone S et al (1995) Successful left trisegmentectomy for ruptured hepatoblastoma using intraoperative transarterial embolization. J Pediatr Surg 30:1709–1712
25. Iida T, Senaga M, Takeuchi Y et al (2004) Successful resection of a ruptured hepatoblastoma prior to chemotherapy: report of a case. Surg Today 34:710–714
26. Hara J, Osugi Y, Ohta H et al (1998) Double-conditioning regimens consisting of thiotepa, melphalan and busulfan with stem cell rescue for the treatment of pediatric tumors. Bone Marrow Transplant 22:7–12
27. Suita S, Tajiri T, Takamatsu H et al (2004) Improved survival outcome for hepatoblastoma based on an optimal chemotherapeutic regimen—a report from the study group for pediatric solid malignant tumors in the Kyushu area. J Pediatr Surg 39:195–198
28. von Schweinitz D, Hecker H, Harmas D et al (1995) Complete resection before development of drug resistance is essential for survival from advanced hepatoblastoma—a report from the German Cooperative Pediatric Liver Tumor Study HB-89. J Pediatr Surg 30:845–852
29. Katzenstein HM, Rigsby C, Shaw PH et al (2002) Novel therapeutic approaches in the treatment of children with hepatoblastoma. J Pediatr Hematol Oncol 24:751–755
30. Palmer RD, Williams DM (2003) Dramatic response of multiply relapsed hepatoblastoma to irinotecan (CPT-11). Med Pediatr Oncol 41:78–80
31. Ijichi O, Ishikawa S, Shinkoda Y et al (2006) Response of heavily treated and relapsed hepatoblastoma in the transplanted liver to single-agent therapy with irinotecan. Pediatr Transplant 10(5):635–638
32. Bomgaars LR, Bernstein M, Krailo M et al (2007) Phase II trial of irinotecan in children with refractory solid tumors: a Children's Oncology Group Study. J Clin Oncol 25:4622–4627
33. Qayed M, Powell C, Morgan ER et al (2010) Irinotecan as maintenance therapy in high-risk hepatoblastoma. Pediatr Blood Cancer 54:761–763

Genome-Wide Analysis of Allelic Imbalances Reveals 4q Deletions as a Poor Prognostic Factor and *MDM4* Amplification at 1q32.1 in Hepatoblastoma

Yasuhito Arai,[1] Shohei Honda,[2] Masayuki Haruta,[2] Fumio Kasai,[2] Yuiko Fujiwara,[2] Junjiro Ohshima,[2] Fumiaki Sasaki,[3] Akira Nakagawara,[3] Hiroshi Horie,[3] Hiroyuki Yamaoka,[3] Eiso Hiyama,[3] and Yasuhiko Kaneko[2,3]*

[1]Cancer Genomics Project, National Cancer Center Research Institute, Chuo-Ku, Tokyo, Japan
[2]Research Institute for Clinical Oncology, Saitama Cancer Center, Ina, Saitama, Japan
[3]Japanese Study Group for Pediatric Liver Tumor (JPLT), Hiroshima, Japan

In a single-nucleotide polymorphism array-based analysis of 56 hepatoblastoma (HB) tumors, allelic imbalances were detected in 37 tumors (66%). Chromosome gains were found in 1q (28 tumors), 2q (24), 6p (8), 8q (8), 17q (6), and 20pq (10), and losses in 1p (6), 4q (9), and 16q (4). Fine mapping delineated the shortest overlapping region (SOR) of gains at 1q32.1 (1.3 Mb) and 2q24.2-q24.3 (4.8 Mb), and losses at 4q34.3-q35.2 (8.7 Mb) and 4q32.3 (1.6 Mb). Uniparental disomy of 11pter-11p15.4 (*IGF2*) and loss of 11pter-p14.1 were found in 11 and 2 tumors, respectively. Expression of *HTATIP2* (11p15.1) was absent in 9 of 20 tumors. Amplification was identified in four tumors at 1q32.1, where the candidate oncogene *MDM4* is located. In the 4q32.3-SRO, *ANXA10S*, a variant of the candidate tumor suppressor *ANXA10*, showed no expression in 19 of 24 tumors. Sequence analysis of *ANXA10S* identified a missense mutation (E36K, c.106G>A) in a HB cell line. Multivariate analysis revealed that both 4q deletion and *RASSF1A* methylation (relative risks: 4.21 and 7.55, respectively) are independent prognostic factors. Our results indicate that allelic imbalances and gene expression patterns provide possible diagnostic and prognostic markers, as well as therapeutic targets in a subset of HB.

INTRODUCTION

Hepatoblastoma (HB) is a rare malignant neoplasm of the liver, with an incidence of 0.5–1.5 per million children (Perilongo and Shafford, 1999). Significant progress in clinical outcome has been achieved in the past 20 years because of advances in chemotherapy and surgical procedures; however, the mortality rate remains 20–30% and treatment results in patients in advanced stages who are refractory to standard preoperative chemotherapy regimens are unsatisfactory (Fuchs et al., 2002). To improve the outcome of these patients, innovative treatment and potent prognostic markers for better therapy planning are needed.

The molecular mechanism involved in the development and progression of HB includes overexpression of insulin-like growth factor-II (*IGF2*) (Li et al., 1998; Honda et al., 2008a), downregulation of *RASSF1A* by promoter hypermethylation (Sugawara et al., 2007; Honda et al., 2008b), and alterations of genes in the Wnt signaling pathway, most notably a high incidence of *CTNNB1* (catenin, beta 1) mutations (Koch et al., 1999).

Cytogenetic and metaphase comparative genomic hybridization (CGH) analyses of HB have revealed frequent occurrence of gains of chromosomes or chromosome arms 1q, 2q, 8q, and 20, and the loss of 4q (Weber et al., 2000; Kumon et al., 2001). More recently, a single-nucleotide polymorphism (SNP) microarray-based analysis of 17 HB samples confirmed these chromosomal gains and losses and identified uniparental disomy (UPD) of 11p (Suzuki et al., 2008).

To narrow down the regions of chromosomal loss or gain detected by previous studies, and to find previously unidentified genetic and epigenetic alterations, we analyzed 56 HB tumors using SNP arrays that can detect both chromosomal aberrations and UPD.

This study demonstrated the shortest overlapping region (SOR) of 1q gain/amplification in 1q32.1 (1.3 Mb) and that of 2q gain in

Supported by: The 3rd-term Comprehensive 10-Year Strategy for Cancer Control from the Ministry of Health, Labor, and Welfare, Japan.

*Correspondence to: Yasuhiko Kaneko, Research Institute for Clinical Oncology, Saitama Cancer Center, 818 Komuro, Ina, Saitama 362-0806, Japan. E-mail: kaneko@cancer-c.pref.saitama.jp

Received 24 December 2009; Accepted 3 March 2010

DOI 10.1002/gcc.20770

Published online 13 April 2010 in Wiley InterScience (www.interscience.wiley.com).

2q24.2-2q24.3 (4.8 Mb). The first SOR of 4q deletion was at 4q34.3-4qter (8.7 Mb), and the second one (1.6 Mb) was at 4q32.3 where *ANXA10* resides. UPD and deletions of 11pter-p14.1 was recurrently found. Expression, mutation, and methylation analyses were carried out in some genes located in the regions mentioned earlier. A survival analysis of patients with HB revealed that 4q deletion (4q- SOR1) is a new prognostic factor indicating a poor outcome. There are several candidate tumor suppressor genes and oncogenes in the SOR regions of 4q loss, 1q32.1 gain/amplification, and 2q gain, and the precise roles of these genes in the tumorigenesis of HB should be clarified.

MATERIALS AND METHODS

Patients and Samples

Tumor tissue specimens were obtained from 56 Japanese children with HB; from 6 of them, samples of adjacent normal tissue or peripheral blood were also available. A second tumor sample was obtained in 2 of the 56 cases; one at initial biopsy and one at surgery in one patient (No. 1), and one each at surgery performed twice in the other (No. 25). The patients underwent biopsy or surgery between March 1989 and September 2004. Data on the status of *IGF2*, *H19*, and *CTNNB1* have previously been reported for 53 of the 56 tumors (Honda et al., 2008a). Three established specimens, including two HB cell lines (HepG2 and HuH6) and one xenografted HB tumor into mice (M194), were also included in the study. DNA and RNA were extracted from the frozen tissues or the cultured cells.

There were 33 males and 23 females, ranging in age from 1 month to 13 years with a median age of 1 year and 6 months. Clinical stage of the disease was determined at the time of initial biopsy or surgery according to the classification of the Japanese Society of Pediatric Surgeons (Hata, 1990). The extent of the disease was stage 1 in 5 tumors, stage 2 in 20, stage 3A in 8, stage 3B in 6, stage 4 in 13, and unknown in four cases. Patients were treated at various hospitals or institutions mostly under the framework of the JPLT-1 (1991–1999) or JPLT-2 (2000–2006) protocols (Sasaki et al., 2002; Matsunaga et al., 2004). The ethics committee of Saitama Cancer Center approved the study design.

Histological Examination

In all tumors, the diagnosis of HB was made with routine hematoxylin- and eosin-stained slides by pathologists at each institution or the JPLT pathology panel according to the classification proposed by the Japanese Pathological Society (1998) and Haas et al. (1989). Pathologists in each institution verified that every sample for molecular genetic analysis contained 70% or more tumor cells.

Copy Number and Loss of Heterozygosity Analysis Using SNP Arrays

High-resolution single-nucleotide polymorphism (SNP) arrays, Affymetrix Mapping 50K-*Xba* and 250K-*Nsp* arrays (Affymetrix, Santa Clara, CA), were used to analyze the chromosomal copy number and loss of heterozygosity (LOH) status in 56 tumors as described previously (Haruta et al., 2008). Partial UPD was defined as a region of copy number-neutral LOH spanning over 3 Mb. Copy numbers and LOH were calculated using CNAG and AsCNAR programs with paired or anonymous references as controls (Nannya et al., 2005; Yamamoto et al., 2007).

Reverse-Transcription (RT)-PCR Analysis of *ANXA10*, *ANXA10S*, *ANP32C*, *ING2*, *FAT1*, and *HTATIP2*

We performed RT-PCR analyses to investigate the expression status of *ANXA10S*, *ANXA10*, *ANXA10S/ANXA10*, *ANP32C*, *ING2*, *FAT1*, and *HTATIP2* in HB tumors and established specimens (Ito et al., 2003; Peng et al., 2005; Wang et al., 2006; Nakaya et al., 2007). PCR primers used for the analysis are listed in Table 1. *ANXA10* consists of 11 exons, and *ANXA10S*, an isoform of *ANXA10*, uses an alternative promoter and encodes a distinct transcript starting from exon 6s (a specific exon consisting of 63 nucleotides in the immediate upstream of exon 6 and 80 nucleotides of exon 6), and ending in exon 11. Primer sequences were obtained from exon 6s and exon 10 for *ANXA10S*, from exon 5 and exon 8 for *ANXA10*, and from exon 9 and exon 11 for both *ANXA10S* and *ANXA10*. *GAPDH* was included as a control for integrity and quantity, and the results of the RT-PCR analysis for six genes were defined as undetectable (−) or detectable (+).

Mutational Analysis of the *ANXA10S* and *HTATIP2* Genes

To detect point mutations and deletions of *ANXA10S* and *HTATIP2*, genomic DNA from

TABLE 1. Primer Sequences Used for RT-PCR, Mutational Analysis, and Methylation-Specific PCR

Primer name	Forward primer sequence	Reverse primer sequence
ING 2 RT1	CATGCAGAGGAACGTGTCTG	CATTTGTCTTGCCCGATTTT
ING 2 RT2	GCGAGAGCTGGACAACAAAT	TTTTCCACCAATTCGAGCAT
ANP32C RT	ATTGCGAGGTAACCAACCTG	TCACGTCCTCCTCTTCACCT CTCACGTCCTCCTCTTCACC
ANXA10 & *10S* RT	TTGTTCTCTGTGTTCGAGACAAACC	GTAGGCAAATTCAGGATAGTAGGC
ANXA10 RT	CCTTAATTCTTTCTGGCTTCACAGT	CAATTCTCATCAGTGCCTACTCCC
ANXA10S RT	CTCAAAACACACTGATACATAGTTC	GGTTTGTCTCGAACACAGAGAACAA
ANXA10S ex6	GGCAGCATTCTGTGGAAATA	TTTGAACATGGCTTCAGTAAATG
ANXA10S ex7	TTCATGAAATCAGGAAATGAACA	ATTTGCAGCATGGTTTTGTG
ANXA10S ex8	CAGGGGACCAGAGAGGAAG	GGCACATCTTATAAACAAAATTCAAA
ANXA10S ex9	TGTTTCAATGGTATTTATAGCAAACAG	TCAGGTTGCCAGTTTAGTGC
ANXA10S ex10	CAAGTGAAAATCTGCATGACTC	CCAGTTTTTCTCACTTGGGTGT
FAT1 RT	CGAGGCATTTGATCCAGATT	TCGGTCTAGCTTCCTTGACG
FAT1 MSP-M[a]	TCGTTTTTTCGTTTTTAGGAAAC	CCAAAAACGTATTTATCCCGAC
FAT1 MSP-U	TTGTTTTTTTGTTTTTAGGAAATGG	CATCCAAAAACATATTTATCCCAAC
HTATIP2 RT	ACTACGCCTCTGCCTTTCAA	GTCACCACAGGCACAGAATG
*HTATIP2*ex3	GGCCTCCCAGCCTGCTAC	GTACTGCCAAATAGCTAG
HTATIP2 MSP-M	TTGAGTTTAGTAGGTGAGGGAAAAC	ACAAAAACGAAACCTAAAAACGA
HTATIP2 MSP-U	TGAGTTTAGTAGGTGAGGGAAAATG	CACAAAAACAAAACCTAAAAACAAA

RT, RT-PCR.
[a]MSP-M and MSP-U, primers for the methylated and unmethylated templates, respectively.

tumors and established specimens was amplified using the primers listed in Table 1. The PCR products were directly sequenced with the BigDye Terminator v3.1 Cycle Sequencing Kit (Applied Biosystems, Foster City, CA).

Methylation-Specific PCR Analysis of the *FAT1* and *HTATIP2* Genes

Genomic DNA from tumors and established specimens was treated with sodium bisulfite, and the methylation status of the promoter region of *FAT1* and *HTATIP2* was analyzed using MSP with the primers listed in Table 1, as previously described (Ito et al., 2003; Nakaya et al., 2007).

Fluorescence In Situ Hybridization Analysis

Fixed cells were prepared from a fresh tumor (No. 26). The BAC clones RP11-284G5 and RP11-433N15 containing *PIK3C2B* and *MDM4*, respectively, were obtained from Rosewell Park Cancer Institute. The copy number of chromosome 1 was examined by D1Z1 (pUC1.77) specific for the 1q pericentromeric region. Probe DNAs were labeled with biotin-16-dUTP or digoxigenin-11-dUTP (Roche) by nick translation. Chromosome painting was performed using the Star*FISH biotin labeled probe (CAMBIO). Hybridization of probes followed standard fluorescence in situ hybridization (FISH) protocols. The hybridization signals were detected by avidin-fluorecein (Roche) for biotin probes or anti-digoxigenin rhodamine (Roche) for digoxigenin probes. The slides were counterstained with Vectashield DAPI (Vector) and examined by fluorescence microscopy equipped with CCD camera (Leica DFC350FX).

Analysis of the Methylation Status of *RASSF1A* and the CTCF6 Site in the *H19*-differentially Methylated Region, and Mutation Analysis of *CTNNB1*

The detailed methods to determine the imprinting status of the *IGF2* gene, *CTNNB1* mutation, and the methylation status of the *RASSF1A* promoter region have been reported previously (Sugawara et al., 2007; Watanabe et al., 2007; Honda et al., 2008b).

Statistical Analysis

Patients were grouped according to biological and clinical features of the disease. The significance of differences in characteristics between the groups was examined using the χ^2 or Fisher's exact test. Overall survival for each group of patients was estimated using the Kaplan–Meier method, and compared using the log-rank test. Time to failure was defined as the interval between surgery or preoperative chemotherapy and death from any cause. The influence of various biological and clinical factors on overall survival was estimated using the Cox proportional-hazards model calculated with the Stat Flex

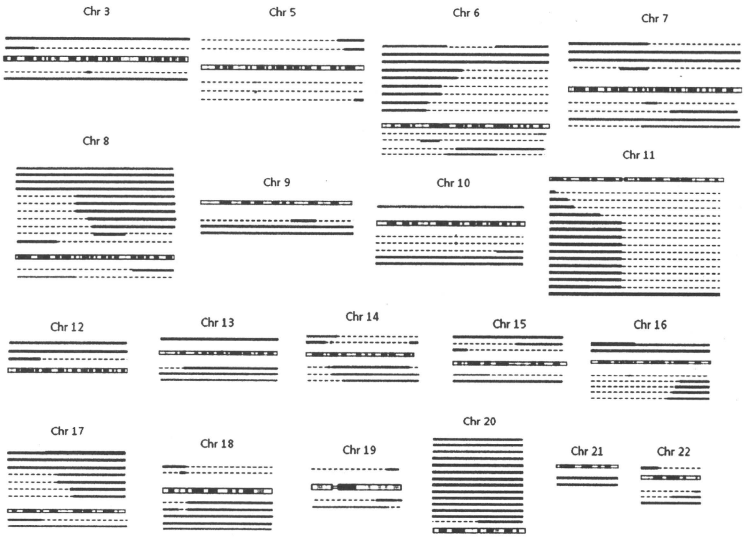

Figure 1. Summary of chromosomal alterations detected by SNP array analyses of 56 HB tumors. Hemizygous deletions (dark blue for tumors and light blue for established specimens) are shown under chromosomes, gains (red for tumors and pink for established specimens) are shown above chromosomes, and UPDs are shown under chromosomes (green for tumors and orange for established specimens). Dotted lines indicate normal chromosome copies. Chr 3, chromosome 3. [Color figure can be viewed in the online issue, which is available at www.interscience.wiley.com.]

software for Windows, version 5.0 (Artec Co., Osaka, Japan).

RESULTS

Chromosomal Aberrations and UPD Regions Detected with SNP Arrays

A SNP array-based analysis was performed on 56 primary HB tumors, two cell lines, and one xenografted tumor. Of the 56 tumors, 37 showed chromosomal gains or losses, whereas 19 showed no chromosomal aberrations. Chromosomal gains of 1q, 2p, 2q, 6p, 8q, 17q, 20p, and 20q and losses of 1p, 4q, and 16q were found in four or more tumors. UPD of 2q and 11p were found in 3 and 11 tumors, respectively (Figs. 1 and 2). In addition, a second tumor sample was obtained in two cases; one sample at first surgery showing 1q+,7q−,+8,11pUPD,17q+,+20 and the other 17 months later at second surgery showing 1q+,2q+,+8,11pUPD,18q−,+20 in one patient (No. 25), and both samples showing 1q+,4q−,11pUPD obtained 7 months apart in the other patient (No. 1). One patient (No. 25) was alive and the other was dead at the last follow-up. Only the aberrations found in the first samples are shown in Figures 1 and 2.

Of the 19 tumors with no chromosomal aberrations, 12 showed LOI of *IGF2*, *RASSF1A* methylation, and/or *CTNNB1* mutation as described below, and seven tumors had no detectable genetic or epigenetic alterations.

Genomic changes were examined with SNP arrays using self-controls in six tumors, and non-self controls consisting of four to eight peripheral blood samples from healthy individuals in 52 tumors. We excluded common copy number variations (CNVs) from the genomic gains and losses found in the present series of HBs by checking a genomic variation database (http://projects.tcag.ca/variation/); however, the possibility that some UPD regions and genomic gains and losses were of germline origin could not be ruled out.

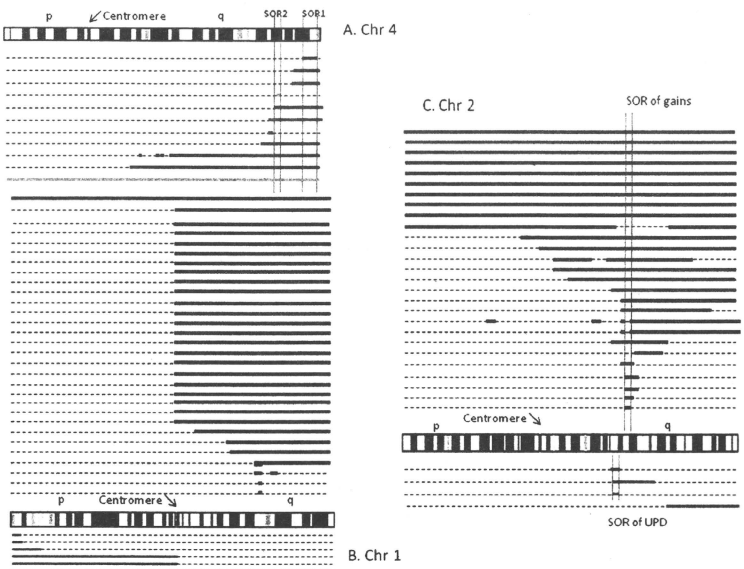

Figure 2. Summary of (A) 4q deletions (dark blue for tumors and light blue for established specimens). The first line below chromosome 4 shows SOR1 of 8.7 Mb found in a tumor (No. 1), and the fourth line shows SOR2 of 1.6 Mb found in the xenograft (M194). (B) 1q gains (red for tumors and pink for established specimens) and 1p deletions (dark blue for tumors). SNP array patterns of four tumors with 1q32.1 amplification are shown in Figure 3. (C) 2q gains (red for tumors and pink for established specimens) and UPDs of 2q (green for tumors and orange for an established specimen). The first line above chromosome 2 shows SOR spanning 4.8 Mb found in a tumor (No. 27). Chr 4, chromosome 4. [Color figure can be viewed in the online issue, which is available at www.interscience.wiley.com.]

Two of the three established specimens showed gains of 1q, 2p, 2q, 8q, 20p, and 20q, one showed a deletion of 4q, and another showed a loss of chromosome 4 (Figs. 1 and 2). All three specimens showed *CTNNB1* mutation, *RASSF1A* methylation, and UPD or LOI of *IGF2*.

1q Gains and 1q32.1 Amplification

As shown in Figure 2, 1q gains were the most frequent allelic imbalance in HB (28 of 56 tumors, 50%; two of three established specimens). Four tumors had genomic amplification limited to 1q32.1 (Fig. 3). Although various CNVs have been reported in the region (http://projects.tcag.ca/variation/), a SNP array analysis using self-controls in one tumor (No. 26) excluded a constitutional origin. Focal amplification of the tumors suggests that the 1q32.1 potentially harbors oncogenes. Karyotypic analysis of one tumor (No. 26) showed double minutes in some metaphase cells, and a subsequent FISH analysis using two BAC probes (RP11-284G5 and RP11-433N15, containing *PIK3C2B* and *MDM4*, respectively) showed amplification of both genes (Fig. 4).

2q Gains

Different sizes of 2q gains were found in 24 tumors and the three established specimens; a whole gain of chromosome 2 in seven tumors and two established specimens, and a partial 2q gain in 17 tumors and one cell line (Fig. 2). A single tumor (No. 27) had the smallest region of 2q gain in 2q24.2-q24.3 (Table 2). Three tumors had the UPD region in 2q, and had a common overlapping region in 2q23.3-q24.1.

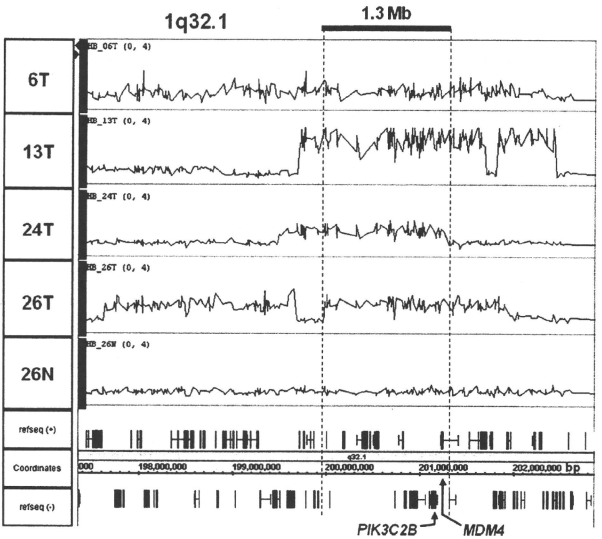

Figure 3. SNP array patters of four tumors (Nos. 6, 13, 24, and 26) with 1q32.1 amplification and self-control of No. 26 are shown. The shortest overlapping region of 1.3 Mb includes *MDM4* and *PIK3C2B*.

4q Deletions

Variously sized 4q deletions were found in nine tumors and two established specimens; a terminal 4q deletion ($n = 7$), an interstitial deletion in the terminal 4q region ($n = 3$), and complete loss of chromosome 4 ($n = 1$) (Fig. 2). Karyotype analysis of the specimen HuH6 with whole loss of chromosome 4 showed a modal chromosome number of 88 with a range between 79 and 91, and a subsequent analysis using a chromosome 4-specific painting probe showed that most cells had three copies of chromosome 4, indicating a loss of chromosome 4 from the tetraploid cells; this was consistent with the results of the SNP array analysis. One tumor (No. 1) had an interstitial deletion of 4q34.3-q35.2 where at least 10 candidate tumor suppressor genes reside (Fig. 2 and Table 2). This region was also deleted in seven other tumors and one cell line, and designated 4q- SOR1. The xenograft had an interstitial deletion in 4q32.3 where *ANXA10* and *PALLD*

Figure 4. Evaluation of *MDM4*/*PIK3C2B* copy number by FISH using RP11-433N15 (red) and RP11-284G5 (green) probes containing *MDM4* and *PIK3C2B*, respectively. Co-amplification of *MDM4*/*PIK3C2B* was identified in an interphase cell of a tumor (No. 26). [Color figure can be viewed in the online issue, which is available at www.interscience.wiley.com.]

TABLE 2. Summary of the Shortest Overlapping Gains/Amplifications, Deletions, and UPD Regions Detected in Hepatoblastoma Tumors

Chromosome region	Shortest overlapping gain/amplification, deletion, and UPD regions (Mb)			Number of tumors with each SOR	Candidate genes in each SOR
	Start	End	Interval		
1q32.1 gain/amplification	199.96	201.31	1.34	28	*MDM4, PIK3C2B, KISS1, SOX13, PRELP*
2q23.3-q24.1UPD	154.23	154.98	0.75	3	*GALNT13*
2q24.2-24.3 gain/amplification	160.69	165.51	4.82	23	*ITGB6, RBMS1, TANK, FAP, IFIH1, GRB14,*
4q32.3 deletion (SOR2)	168.63	170.27	1.64	5	*ANXA10S, PALLD*
4q34.3-q35.2 deletion (SOR1)	181.34	190.01	8.67	8	*ING2, IRF2, CASP3, MLF1IP, SNX25, SORBS2, TLR3, MTNR1A, FAT1, FSHD*
16q23.1-qter deletion	75.58	88.36	12.77	4	*WWOX, CDH15, FANCA*

UPD, uniparental disomy; SOR, the shortest overlapping region.

reside (Fig. 2 and Table 2). This region was also deleted in five tumors and one cell line (4q-SOR2; Fig. 2). One tumor (No. 28) had an interstitial deletion in 4q32.2 (165.1–165.9 Mb; 814 kb) where *ANP32C* is located (Fig. 2). This region was deleted in three other tumors and one cell line.

UPD and LOI of IGF2 and 11p15 Deletion

The results of the LOH and LOI analyses of the *IGF2-H19* region have been reported previously (Honda et al., 2008a). SNP array analysis revealed UPD in 11p in 11 tumors and two established specimens (Fig. 1). UPD in all 13 samples included *IGF2* at 11p15.5. One tumor (No. 29) had a loss of 11pter-p14.1 and UPD in 11p14.1-cen, suggesting the occurrence of UPD of whole 11p followed by the loss of 11pter-p14.1. Another tumor (No. 7) had a complete loss of chromosome 11.

All 13 samples with UPD including the *IGF2-H19* region had a hypermethylated CTCF6, indicating duplication of the paternal allele. Two tumors with a loss of 11p15 or whole chromosome 11 showed hypermethylated CTCF6, indicating the paternal origin of the remaining allele. In addition, 10 tumors with retention of heterozygosity (ROH) of *IGF2* had hypermethylated CTCF6, indicating LOI of *IGF2*. Thus, *IGF2* alterations, including UPD and LOI, were found in 21 of 56 (37.5%) tumors.

Analysis of Candidate Tumor Suppressor Genes Located in the 4q Deletion Region

ANXA10, located in a small interstitial deletion region of the xenograft, and *ANXA10S* is an isoform of *ANXA10*. The primer sequences from exons 9 and 11 detect both *ANXA10* and *ANXA10S* transcripts. The *ANXA10*/*ANXA10S* transcripts were expressed in fetal and normal liver tissues, all 11 tumors examined, and the xenograft, but not in the two cell lines. In contrast, *ANXA10S* was not expressed in 19 of 24 tumors and the three established specimens, but expressed in fetal and normal liver tissues and five tumors (Fig. 5 and Table 3). In addition, *ANXA10* was expressed in five tumors, but not in six tumors and the three established specimens. We examined the sequences of *ANXA10S* (AY626137) in 24 tumors and the established specimens. One cell line (HuH6) showed a hemizygous missense mutation in exon 7 (E36K, c.106G>A), and three tumors had two synonymous sequence alterations; exon 6s (S20S, c.60A>G) in Nos. 19 and 21, and exon 8 (L79L, c.235C>T) in No. 15 (Fig. 5). The nucleotide change in exon 6, but not that in exon 7 or 8, has been reported as a SNP in the dbSNP database (NCBI, build 130).

ANP32C, located in a small interstitial deletion region of one tumor (No. 28), was expressed in all 13 tumors examined and the two cell lines with or without 4q deletion; RNA was not available for analysis in the tumor 28 (Table 3). *ING2* and *FAT1* reside in 4q35.1 (184.6 and 187.8 Mb, respectively), and both genes were included in the common deletion region (4q-SOR1) of eight tumors and one cell line (HuH6). *ING2* was expressed in fetal and normal liver tissues and all 13 tumors with or without 4q deletion. *FAT1* was expressed in fetal and normal liver tissues and 11 tumors and the two cell lines with and without 4q deletion, but not in three tumors with normal 4q (Nos. 6, 12, and 17) (Table 3). MSP analysis of *FAT1* showed an unmethylated promoter region in all 24 tumors and three established specimens regardless of the status of *FAT1*

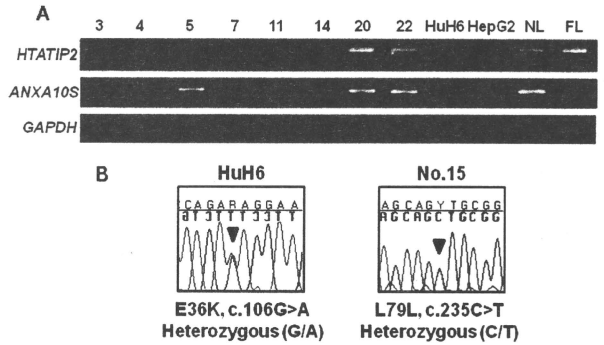

Figure 5. (A) RT-PCR analysis of the *HTATIP2* and *ANXA10S* genes in eight HB tumors, two HB cell lines (HuH6 and HepG2), and normal and fetal liver tissues (NL and FL). *GAPDH* was included as a control for integrity and quantity (lower panel). The expression status of *HTATIP2* and *ANXA10S* is also shown in Table 3. (B) Sequence analysis of *ANXA10S* (GenBank: AY626137). One cell line, HuH6, showed a missense mutation in exon 7 (c.106G>A, E36K), and one tumor (No. 15) had a SNP in exon 8 (c.235C>T, L79L). [Color figure can be viewed in the online issue, which is available at www.interscience.wiley.com.]

expression or 4q deletion (Table 3). Thus, both *ING2* and *FAT1* are unlikely to be involved in the tumorigenesis of HB.

Analysis of *HTATIP2* Located in 11p15.1

Two tumors had loss of 11pter-p14.1, suggesting the presence of tumor suppressor gene(s) but not growth promoting gene(s) such as *IGF2*. *HTATIP2* at 11p15.1 is included in the deleted region, and reported as a candidate tumor suppressor gene for hepatocellular carcinoma (Ito et al., 2003). *HTATIP2* was expressed in fetal and normal liver tissues and 11 tumors, but not in nine tumors and the two cell lines, including one (No. 7) with loss of chromosome 11 (Table 3 and Fig. 5). MSP analysis of *HTATIP2* showed the promoter region to be methylated in both cell lines, but unmethylated in all 24 tumors regardless of the expression status. Subsequent sequencing of *HTATIP2* showed no mutation in the 19 tumors and three established specimens. Thus, the involvement of *HTATIP2* in the tumorigenesis cannot be excluded at present.

Mutation and Deletion of *CTNNB1*

Of 51 tumors examined, 12 had point mutations in exon 3 of *CTNNB1*, 24 had deletions of various sizes ranging from 19 to 591 bp, always including exon 3, and 15 had no mutations and deletions as reported previously (Honda et al., 2008a). Tumor DNA was not available for analysis in the other five tumors.

Quantitative MSP Analysis of *RASSF1A* Methylation

A quantitative MSP analysis was performed in 56 tumors, three established specimens, and five adjacent normal liver specimens. We adopted a cutoff value of 4.8% used for the previous study (Honda et al., 2008b). Hypermethylation of the *RASSF1A* promoter region was detected in 26 (46.4%) of 56 tumors and in all three established specimens. All five adjacent normal tissue specimens showed unmethylated *RASSF1A*.

Preoperative Chemotherapy Did Not Affect the Incidence of *IGF2*-LOI, *CTNNB1* Mutations, *RASSF1A* Methylation, and Chromosomal Aberrations

Of 56 tumors, 39 and 15 were treated with and without preoperative chemotherapy, respectively; therapy status was unknown for two tumors. *IGF2*-LOI, *RASSF1A* methylation, and chromosomal aberrations were found in 5 (12.3%), 20 (51.3%), and 22 (56.4%), respectively, of the 39 treated tumors, and in 4 (26.7%), 5 (33.3%), and 12 (80.0%), respectively, of the 15 untreated tumors. In addition, *CTNNB1* mutations were found in 23 (65.7%) of 35 treated tumors, and in

TABLE 3. Expression, Mutation, and Methylation Analyses of Genes Located in the Terminal 4q or 11p15 Deletion Regions in Hepatoblastoma Tumors and Established Specimens

Samples	4q or 11p status	*ANXA10S* (4q32.3)	*ANXA10S* sequences	*ANXA10* (4q32.3)	*ANXA10/10S* (4q32.3)	*ANP32C* (4q32.3)	*ING2* (4q35.1)	*FAT1* (4q35.1)	*FAT1* MSP	*HTATIP2* (11p15.1)	*HTATIP2* MSP	*HTATIP2* sequences
Tumors (n = 24)												
1	del(4)(q34.3q35.2), UPD11p	−	Normal	+	+	+	+	+	U	+	U	Normal
2	del(4)(q13.3)	−	ND	ND	ND	ND	ND	ND	U	−	U	Normal
3	Normal	−	Normal	−	+	+	+	+	U	+	U	Normal
4	Normal	−	Normal	−	+	+	+	+	U	+	U	Normal
5	Normal	+	Normal	ND	ND	ND	ND	ND	U	+	U	Normal
6	Normal	−	Normal	ND	ND	ND	ND	−	U	+	U	Normal
7	Loss of chromosome 11	−	Normal	+	+	+	+	+	U	−	U	Normal
8	Normal	−	Normal	+	+	+	+	+	U	+	U	Normal
9	Normal	−	Normal	+	+	+	+	+	U	+	U	Normal
10	Normal	−	Normal	ND	ND	ND	ND	ND	U	ND	U	Normal
11	Normal	−	Normal	+	+	+	+	+	U	−	U	Normal
12	UPD11p	−	Normal	ND	ND	+	+	−	U	−	U	Normal
13	Normal	−	ND	ND	ND	+	+	ND	U	−	U	Normal
14	Normal	+	Normal	ND	ND	ND	ND	ND	U	−	U	Normal
15	UPD11p	−	SNP (exon 8)[a]	−	+	+	+	+	U	+	U	Normal
16	Normal	+	Normal	ND	ND	ND	ND	ND	U	−	U	Normal
17	Normal	−	Normal	−	+	+	+	−	U	−	U	Normal
18	Normal	−	Normal	−	+	+	+	+	U	−	U	Normal
19	Normal	−	SNP (exon 6s)[b]	ND	ND	ND	ND	+	U	ND	U	ND
20	Normal	+	Normal	ND	ND	ND	ND	ND	U	+	U	ND
21	Normal	−	SNP (exon 6s)[b]	ND	ND	ND	ND	ND	U	ND	U	ND
22	Normal	+	Normal	ND	ND	ND	ND	ND	U	+	U	ND
23	Normal	−	Normal	−	+	+	+	+	U	+	U	Normal
24	Normal	−	Normal	ND	ND	ND	ND	ND	U	ND	U	ND
Established specimens (one xenograft, M194, and 2 cell lines)												
M194	del(4)(q32.3q32.3), UPD11p	−	Normal	−	+	ND	ND	ND	U	+	U	Normal
HuH6	Loss of chromosome 4	−	Missense M.[c]	−	−	+	+	+	U	−	M	Normal
HepG2	UPD11p	−	Normal	−	−	+	+	+	U	−	M	Normal
Normal tissues												
202N/15N	Not relevant	+	Not relevant	+	+	ND	+	+		+		
M299N/19N	Not relevant	+	Not relevant	+	+	ND	ND	+		+		
Fetal liver	Not relevant	+	Not relevant	+	+	+	+	+		+		

MSP, methylation-specific PCR; del, deletion; UPD11p, uniparental disomy of 11p; U, unmethylated; M, methylated; ND, not done; −, expression undetectable; +, expression detectable; Missense M., missense mutation.

[a]c.235C>T, L79L.

[b]c.60A>G, S20S.

[c]c.106G>A, E36K.

TABLE 4. Clinical, Genetic, and Epigenetic Characteristics in Hepatoblastoma Tumors with or without 4q Deletion

		4q deletion	No 4q deletion	*P* value
Total number of patients (n=56)		8 (14.3%)	48 (85.7%)	
Age at diagnosis ($n = 54$)	<2 years	4 (50%)	30 (65.2%)	0.410
	≥2 years	4 (50%)	16 (34.8%)	
Sex ($n = 56$)	Male	4 (50%)	29 (60.4%)	0.307
	Female	4 (50%)	19 (39.6%)	
Stage ($n = 52$)	1, 2, 3A	3 (37.5%)	30 (68.2%)	0.097
	3B, 4	5 (62.5%)	14 (31.8%)	
Outcome ($n = 53$)	Died	5 (62.5%)	10 (27.1%)	0.019
	Alive	3 (37.5%)	35 (72.9%)	
Status of *RASSF1A* ($n = 56$)	Methylated	4 (50%)	22 (45.8%)	0.826
	Unmethylated	4 (50%)	26 (54.2%)	
Status of *CTNNB1* ($n = 51$)	Mutated	7 (88%)	29 (67.4%)	0.252
	Not mutated	1 (12%)	14 (32.6%)	
Status of *IGF2* ($n = 56$)	UPD	3 (37.5%)	8 (16.7%)	0.169
	No UPD	5 (62.5%)	40 (83.3%)	
Status of *IGF2* ($n = 54$)	UPD	3 (37.5%)	8 (17.4%)	0.212
	LOI	0	10 (21.7%)	
	ROI	5 (62.5%)	28 (60.9%)	

UPD, uniparental disomy; LOI, loss of imprinting; ROI, retention of imprinting.

11 (78.6%) of 14 untreated tumors. There was no significant difference in the incidence of *IGF2*-LOI, *RASSF1A* methylation, chromosomal aberrations or *CTNNB1* mutations between the treated and untreated tumors ($P = 0.22$, $P = 0.24$, $P = 0.11$, and $P = 0.38$, respectively). These results indicate that preoperative chemotherapy did not affect the incidences of the genetic and epigenetic alterations.

Clinical, Genetic, and Epigenetic Characteristics of Hepatoblastoma Tumors with or without the Terminal 4q Deletion

There were no significant differences in age and the ratio of boys to girls between 8 patients with 4q deletions (SOR1) and 46 patients with no 4q deletion (Table 4). Cases with terminal 4q deletions tended to be at a more advanced stage ($P = 0.097$), and had a poorer outcome ($P = 0.019$) than cases with no terminal 4q deletions. In addition, there was no significant difference in the incidence of *RASSF1A* methylation, *CTNNB1* mutations, *IGF2*-UPD, and *IGF2*-LOI between patients with or without 4q deletions (Table 4).

Overall Survival of Patients Classified by Clinical and Biological Characteristics

We evaluated the association of clinical and biological characteristics with overall survival in 48 patients with HB; 8 patients were excluded because of a lack of data. Patients less than 2 years of age showed better overall survival than those 2 years old or more ($P = 0.013$) (Fig. 6). Likewise, patients with a stage 1, 2, or 3A tumor showed better overall survival than those with a stage 3B or 4 tumor ($P = 0.015$). Patients with a tumor with unmethylated *RASSF1A*, normal 4q, or normal 16q showed better overall survival than those with a tumor with methylated *RASSF1A*, 4q deletion, or 16q deletion ($P = 0.001$, $P = 0.007$, or $P = 0.022$), respectively. Patients with a tumor with normal 1q or normal 4q32.3 (*ANXA10*) tended to show better overall survival than those with a tumor with 1q gain or 4q32.3 deletion ($P = 0.069$ or $P = 0.061$), respectively. There were no differences in overall survival times between males and females, or between patients with a tumor with *IGF2* alteration (UPD or LOI) and with a tumor without *IGF2* alteration. In addition, chromosomal aberrations, including 1p deletion, 2q gain, 6p gain, 8q gain, 17q gain, and 20q gain, did not affect overall survival.

A multivariate Cox proportional hazard regression analysis was performed using five factors that showed differences in outcome by a univariate analysis. Intriguingly, *RASSF1A* methylation and 4q deletion indicated a poor outcome, but age of the patients, stage of the disease, or 16q deletion did not (Table 5).

DISCUSSION

Previous cytogenetic and metaphase CGH studies of HB have revealed frequent occurrence of gains of 1q, 2q, 8q, 20p, and 20q, and losses of

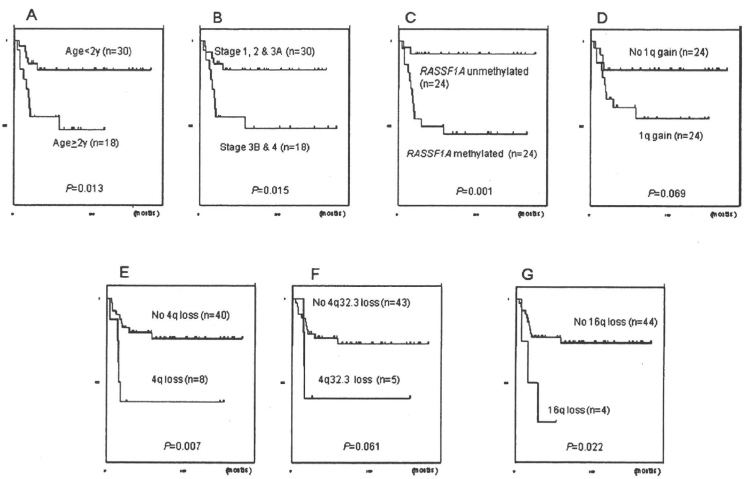

Figure 6. Overall survival curves for HB patients based on different variables: (A) age, (B) disease stage, (C) methylation status of the *RASSF1A* gene, (D) 1q gain, (E) 4q loss, (F) 4q32.3 (*ANXA10*) loss, and (G) 16q loss.

TABLE 5. Multivariate Analysis of Five Clinicopathological and Genetic Factors in 48 Patients with Hepatoblastoma

Prognostic factors	Relative risk (95% CI)	*P* value	Relative risk (95% CI)	*P* value
Age				
<2 year versus ≥2 year	1.93 (0.58–6.21)	0.280	2.12 (0.67–6.75)	0.200
Stage				
1, 2, 3A versus 3B, 4	1.46 (0.41–5.25)	0.554	2.14 (0.66–6.85)	0.199
4q deletion				
Absent versus present	4.21 (1.13–15.58)	0.031		
16q deletion				
Absent versus present			2.79 (0.72–10.74)	0.133
RASSF1A				
Unmethylated versus methylated	7.58 (1.08–82.06)	0.012	5.76 (1.23–27.02)	0.026

CI, confidence interval.

4q (Weber et al., 2000; Kumon et al., 2001). The present analysis of tumor samples using SNP arrays allowed us to narrow down these specific regions of chromosomal gains and losses.

The most frequently gained region was 1q, and a novel genomic amplification was identified in 1q32.1 (1.3 Mb), seen in four tumors (Figs. 3 and 4). Subsequent FISH analyses identified *MDM4* and *PIK3C2B* to be co-amplified in one of the four tumors. Previous studies have reported *MDM4* and *PIK3C2B* to be amplified in many tumor types, including glioblastoma, hepatocellular carcinoma, and retinoblastoma, although not in HB (Riemenschneider et al., 1999; Zielinski et al., 2005; Schlaeger et al., 2008). Of the patients with 1q32.1 amplification, two have died, one is alive, and one is unknown as regards outcome. Anticancer drugs targeting *MDM4* and *PIK3C2B* are being developed (Traer et al., 2006; Toledo and Wahl, 2007), and this study indicates that such drugs should be tried to treat refractory HB with 1q32.1 amplification.

Terminal 4q is the most common region for deletion in HB tumors, and the SOR1 was identified in 4q34.3-q35.2 (8.7 Mb), involved in eight

tumors (Fig. 2). The candidate tumor suppressor genes located in SOR1 are listed in Table 2 (NCBI database). Frequent LOH in the 4q terminal region has been reported in hepatocellular carcinoma, head and neck squamous cell carcinoma, and oral carcinoma (Midorikawa et al., 2006; Nakaya et al., 2007; Nakamura et al., 2008). *FAT1* (4q35.1) is a new member of the human cadherin superfamily and was originally discovered in Drosophila, where it is thought to function as a tumor suppressor. Nakaya et al. (2007) found frequent exonic homozygous deletions of *FAT1* in primary oral cancers and cell lines, and that hypermethylation of the CpG islands of the *FAT1* promoter region inversely correlated with its expression in oral squamous cell carcinoma cell lines. However, this study showed that *FAT1* was expressed in the great majority of tumors, and its promoter region was unmethylated in all tumors regardless of the expression. Thus, *FAT1* is unlikely to be the target gene for the terminal 4q deletion in HB.

Another candidate tumor suppressor gene in the terminal 4q region is *ING2*, which has been shown to be involved in the regulation of gene transcription, cell cycle arrest, and apoptosis in a *TP53*-dependent manner for maintaining genomic stability (Wang et al., 2006). Its reduced expression has been reported in primary melanoma tumors and lung cancer cell lines, although mutation in the *ING2* gene has been rarely reported (Lu et al., 2006). In the present series of HB tumors and cell lines, all samples showed *ING2* mRNA expression; these findings suggest no involvement of *ING2* in the tumorigenesis of HB. Expression, methylation, and mutational analyses are required for the other eight genes.

ANXA10, a member of the annexin family of calcium-dependent phospholipid-binding proteins, was located in a small interstitially deleted region of the xenograft (SOR2 of 4q deletion) (Fig. 2). It has previously been reported that *ANXA10S*, a short isoform of *ANXA10*, is expressed in adult liver and downregulated in most hepatocellular carcinomas (Peng et al., 2005). *ANXA10S* downregulation correlated with high-grade and high-stage hepatocellular carcinoma, early recurrence, and lower 10-year survival. More recently, downregulation of *ANXA10* and its correlation with poor survival was reported in gastric cancer (Kim et al., 2009). These findings suggest *ANXA10* or *ANXA10S* to be a tumor suppressor gene. This study also showed downregulation of *ANXA10S* in the great majority of HB tumors, and downregulation of *ANXA10* in some HB tumors. Furthermore, a hemizygous missense mutation of *ANXA10S* in the HuH6 cell line, resulting in an amino acid substitution (E36K; from glutamic acid to lysine), and a small hemizygous interstitial deletion spanning *ANXA10* in a xenograft suggest that it is a candidate tumor suppressor gene, although the xenograft showed normal *ANXA10S* sequences in the remaining allele. Haploinsufficiency for tumor suppression is reported in *DMP1* and *PTEN* (Inoue et al., 2001; Kown et al., 2008), and the present findings suggest that down-regulation and hemizygous mutation or deletion of *ANXA10*/*ANXA10S* play some roles in the progression of HB.

ANP32C, acidic leucine-rich nuclear phosphoprotein 32, member C, is expressed in prostate cancer and is tumorigenic when stably transfected into NIH3T3 cells (Kadkol et al., 1999). One tumor (No. 28) had a small interstitial deletion of 814 kb at 4q32.2, including *ANP32C*. All 13 HB tumors and two cell lines expressed *ANP32C*, suggesting that this gene is unlikely to be a tumor suppressor gene.

A single tumor (No. 27) had the smallest region of 2q gain in 2q24.2-q24.3 where at least six candidate oncogenes reside (Table 2). Two tumor samples were obtained from one patient (No. 25). The first sample showed no 2q gain, whereas the second obtained 17 months later showed 2q gain, including 2q24.2-q24.3, indicating the gain to be associated with HB progression. Three tumors shared an overlapping UPD region in 2q23.3-2q24.1 (Fig. 2B), and *GALNT13*, encoding a glycosyltransferase that initiates mucin-type *O*-glycosylation (Berois et al., 2006), is the only gene located in this UPD region. *GALNT13* transcripts are expressed in bone marrow neuroblastoma cells and in oligodendrogliomas with 1p19q codeletions (Ducray et al., 2008). A molecular analysis of some of the genes located in the SOR of 2q gain or UPD may clarify their roles in the tumorigenesis of HB.

IGF2 is an imprinted gene with paternal expression and encodes a fetal growth factor (Foulstone et al., 2005). Overexpression of *Igf2* in mouse fetuses causes overgrowth of many organs, including liver and kidney, and plays a crucial role in the development of many embryonal tumors. This study showed UPD of *IGF2* in 11 HB tumors (Fig. 1), and loss of 11pter-p14.1 in two tumors. In addition, LOI of *IGF2* was found in 10 tumors, indicating *IGF2* alterations in 21

(37.5%) of 56 HB tumors. We previously reported that most HB tumors with UPD or LOI of *IGF2* have elevated levels of *IGF2* mRNA (Honda et al., 2008a). These findings suggest that UPD of the *IGF2* (11p15.5) region has a role to duplicate the paternal copy of *IGF2*, resulting in overexpression that may contribute to the proliferation of the HB precursor cells.

On the other hand, two tumors had loss of the 11p terminal region; this region overlapped with the UPD region of many tumors with 11p UPD. These findings also suggest that there may be tumor suppressor genes in the deleted region. We analyzed the expression, mutation, and methylation status of *HTATIP2*, a candidate tumor suppressor gene for hepatocellular carcinoma, located at 11p15.1 (Ito et al., 2003). While the downregulation of *HTATIP2* was observed both in some hepatocellular carcinomas or HB tumors, somatic mutations were observed only in hepatocellular carcinoma. In addition, the promoter region of *HTATIP2* was unmethylated in 28 HB tumors with or without 11p15.1 alterations, and there was no difference in the expression status of *HTATIP2* between four tumors with 11p15.1 loss or UPD and 16 tumors without 11p15.1 loss or UPD. From these findings, there is not enough evidence supporting that *HTATIP2* is involved in the tumorigenesis of HB.

To improve the outcome of patients with HB who are refractory to standard preoperative chemotherapy regimens, effective prognostic markers for better treatment planning are needed. We previously reported that methylation status of the *RASSF1A* promoter region is a promising molecular-genetic marker predicting treatment outcome (Honda et al., 2008b). In a univariate analysis, we found that 4q and 16q deletions and possibly also 1q gain and 4q32.3 (*ANXA10*) loss were predictive of a poor outcome (Fig. 6). Downregulation of *ANXA10* or *ANXA10S* expression may play some roles in the aggressive nature of HB as reported in hepatocellular carcinoma and gastric cancer (Peng et al., 2005; Kim et al., 2009). Of 10 genes in the 4q terminal region, two genes, *ING2* and *FAT1*, could be excluded as candidates for a tumor suppressor gene in HB based on this study. LOH at 16q was reported as an adverse prognostic factor for Wilms tumor (Grundy et al., 2005). Because HB and Wilms' tumor are derived from embryonal cells and share UPD and LOI of *IGF2* (Honda et al., 2008a), the same tumor suppressor gene in 16q may be involved in the tumorigenesis of both.

The multivariate analysis showed that *RASSF1A* methylation and the terminal 4q deletion (SOR1) but not 16q deletion or 1q gain are independent prognostic factors. Tumors with the terminal 4q deletion tended to be at a more advanced stage than tumors with no deletion, but did not show any specific clinical, genetic, or epigenetic characteristics (Table 4). We previously proposed that *RASSF1A* may be a promising molecular-genetic marker to predict treatment outcome, and that it may be used to stratify patients when clinical trials are carried out (Honda et al., 2008b). Of eight cases with the terminal 4q deletion, four with methylated *RASSF1A* and one with unmethylated *RASSF1A* died of the disease. The addition of 4q deletion to *RASSF1A* methylation may be more useful to stratify patients with HB for better therapy planning.

In summary, the analysis of copy number and UPD using high-density SNP arrays in 56 HB samples revealed pathologically relevant regions of allelic imbalance, suggesting involvement of tumor suppressor genes and/or oncogenes. Stratification of the patients by these genomic changes and targeted therapies will be beneficial when the precise roles of these genes in the tumorigenesis of HB are verified.

ACKNOWLEDGMENTS

We express our gratitude to the physicians participating in the Japanese Study Group for Pediatric Liver Tumor (JPLT) who supplied samples and clinical data for this study.

REFERENCES

Berois N, Blanc E, Ripoche H, Mergui X, Trajtenberg F, Cantais S, Barrois M, Dessen P, Kågedal B, Bénard J, Osinaga E, Raguénez G. 2006. ppGalNAc-T13: A new molecular marker of bone marrow involvement in neuroblastoma. Clin Chem 52:1701–1712.

Ducray F, Idbaih A, de Reyniès A, Bièche I, Thillet J, Mokhtari K, Lair S, Marie Y, Paris S, Vidaud M, Hoang-Xuan K, Delattre O, Delattre JY, Sanson M. 2008. Anaplastic oligodendrogliomas with 1p19q codeletion have a proneural gene expression profile. Mol Cancer 7:41.

Foulstone E, Prince S, Zaccheo O, Burns JL, Harper J, Jacobs C, Church D, Hassan AB. 2005. Insulin-like growth factor ligands, receptors, and binding proteins in cancer. J Pathol 205:145–153.

Fuchs J, Rydzynski J, Von Schweinitz D, Bode U, Hecker H, Weinel P, Burger D, Harms D, Erttmann R, Oldhafer K, Mildenberger H. 2002. Pretreatment prognostic factors and treatment results in children with hepatoblastoma. Cancer 95:172–182.

Grundy PE, Breslow NE, Li S, Perlman E, Beckwith JB, Ritchey ML, Shamberger RC, Haase GM, D'Angil GJ, Donaldson M, Coppes MJ, Malogolowkin M, Shearer pThomas PR, Macklis R, Tomlinson G, Huff V, Green DM. 2005. Loss of heterozygosity for chromosomes 1p and 16q is an adverse prognostic factor in favorable-histology Wilms tumor: A report from the National Wilms Tumor Study Group. J Clin Oncol 23:7312–7321.

Haas JE, Muczynski KA, Krailo M, Ablin A, Land V, Vietti TJ, Hammond GD. 1989. Histopathology and prognosis in childhood hepatoblastoma and hepatocarcinoma. Cancer 64:1082–1095.

Haruta M, Arai Y, Sugawara W, Watanabe N, Honda S, Ohshima J, Soejima H, Nakadate H, Okita H, Hata J, Fukuzawa M, Kaneko Y. 2008. Duplication of paternal *IGF2* or loss of maternal *IGF2* imprinting occurs in half of Wilms tumors with various structural *WT1* abnormalities. Genes Chromosomes Cancer 47:712–727.

Hata Y. 1990. The clinical features and prognosis of hepatoblastoma: Follow-up studies done on pediatric tumors enrolled in the Japanese Pediatric Tumor Registry between 1971 and 1980. Jpn J Surg 20:498–502.

Honda S, Arai Y, Haruta M, Sasaki F, Ohira M, Yamaoka H, Horie H, Nakagawara A, Hiyama E, Todo S, Kaneko Y. 2008a. Loss of imprinting of *IGF2* correlates with hypermethylation of the *H19* differentially methylated region in hepatoblastoma. Brit J Cancer 99:1891–1899.

Honda S, Haruta M, Sugawara W, Sasaki F, Ohira M, Matsunaga T, Yamaoka H, Horie H, Ohnuma N, Nakagawara A, Hiyama E, Todo S, Kaneko Y. 2008b. The methylation status of *RASSF1A* promoter predicts responsiveness to chemotherapy and eventual cure in hepatoblastoma patients. Int J Cancer 123:1117–1125.

Inoue K, Zindy f, Randle DH, Rehg JE, Sherr CJ. 2001. *Dmp1* is haploinsufficient for tumor suppression and modifies the frequencies of *Arf* and *p53* mutation in *Myc*-induced lymphomas. Genes Dev 15:2934–2939.

Ito M, Jiang C, Krumm K, Zhang X, Pecha J, Zhao J, Guo Y, Roeder RG, Xiao H. 2003. TIP30 deficiency increases susceptibility to tumorigenesis. Cancer Res 63:8763–8767.

Japanese Society of Pathology. 1998. Committee on histological classification of childhood tumors. Histological Classification and Atlas of Tumors in Infancy and Childhood. IV. Tumors of the liver, Gallbladder and Pancreas, 1st ed. Tokyo, Kanahara Shuppan.

Kadkol S, Brody JR, Pevsner J, Bai J, Pasternack GR. 1999. Modulation of oncogenic potential by alternative gene use in human prostate cancer. Nat Med 5:275–279.

Kim J, Kim MA, Jee CD, Jung EJ, Kim WH. 2009. Reduced expression and homozygous deletion of annexin A10 in gastric carcinoma. Int J Cancer 125:1842–1850.

Koch A, Denkhaus D, Albrecht S, Leuschner I, Von Schweinitz D, Pietsch T. 1999. Childhood hepatoblastomas frequently carry a mutated degradation targeting box of the β-catenin gene. Cancer Res 59:269–273.

Kown CH, Zhao D, Chen J, Alcantara S, Li Y, Bums DK, Mason RP, Lee EY, Wu H, Parada LF. 2008. *Pten* haploinsufficiency accelerates formation of high-grade astrocytomas. Cancer Res 68:3286–3294.

Kumon K, Kobayashi H, Namiki T, Tsunematsu Y, Miyauchi J, Kikuta A, Horikoshi Y, Komada Y, Hatae Y, Eguchi H, Kaneko Y. 2001. Frequent increase of DNA copy number in the 2q24 chromosomal region and its association with a poor clinical outcome in hepatoblastoma: Cytogenetic and comparative genomic hybridization analysis. Jpn J Cancer Res 92:854–862.

Li X, Kogner P, Sandstedt B, Haas OA, Ekström TJ. 1998. Promoter-specific methylation and expression alterations of *igf2* and *h19* are involved in human hepatoblastoma. Int J Cancer 75:176–180.

Lu F, Dai DL, Martinka M, Ho V, Li G. 2006. Nuclear ING2 expression is reduced in human cutaneous melanomas. Br J Cancer 95:80–86.

Matsunaga T, Sasaki F, Ohira M, Hashizume K, Hayashi A, Hayashi Y, Matsuyama T, Mugishima H, Ohnuma N. 2004. The role of surgery in the multimodal treatment for hepatoblastomas. Shounigan 41:205–210 (in Japanese).

Midorikawa Y, Yamamoto S, Ishikawa S, Kamimura N, Igarashi H, Sugimura H, Makuuchi M, Aburatani H. 2006. Molecular karyotyping of human hepatocellular carcinoma using single-nucleotide polymorphism arrays. Oncogene 25:5581–5890.

Nakamura E, Kozaki K, Tsuda H, Suzuki E, Pimkhaokham A, Yamamoto G, Irie T, Tachikawa T, Amagasa T, Inazawa J, Imoto I. 2008. Frequent silencing of a putative tumor suppressor gene melatonin receptor 1 A (*MTNR1A*) in oral squamous-cell carcinoma. Cancer Sci 99:1390–1400.

Nakaya K, Yamagata HD, Arita N, Nakashiro KI, Nose M, Miki T, Hamakawa H. 2007. Identification of homozygous deletions of tumor suppressor gene *FAT* in oral cancer using CGH-array. Oncogene 26:5300–5308.

Nannya Y, Sanada S, Nakazaki K, Hosoya N, Wang L, Hangaishi A, Kurokawa M, Chiba S, Bailey DK, Kennedy GC, Ogawa S. 2005. A robust algorithm for copy number detection using high-density oligonucleotide single nucleotide polymorphism genotyping arrays. Cancer Res 65:6071–6079.

Peng SY, Ou YH, Chen WJ, Li HY, Liu SH, Pan HW, Lai PL, Jeng YM, Chen DC, Hsu HC. 2005. Aberrant expressions of annexin A10 short isoform, osteopontin and alpha-fetoprotein at chromosome 4q cooperatively contribute to progression and poor prognosis of hepatocellular carcinoma. Int J Oncol 26:1053–1061.

Perilongo G, Shafford EA. 1999. Liver tumours. Eur J Cancer 35:953–958.

Riemenschneider MJ, Büschges R, Wolter M, Reifenberger J, Boström J, Kraus JA, Schlegel U, Reifenberger G. 1999. Amplification and overexpression of the *MDM4* (*MDMX*) gene from 1q32 in a subset of malignant gliomas without *TP53* mutation or *MDM2* amplification. Cancer Res 59:6091–6096.

Sasaki F, Matsunaga T, Iwafuchi M, Hayashi Y, Ohkawa H, Ohira M, Okamatsu T, Sugito T, Tsuchida Y, Toyosaka A, Nagahara N, Nishihira H, Hata Y, Uchino J, Misugi K, Ohnuma N. 2002. Outcome of hepatoblastoma treated with the JPLT-1 (Japanese Study Group for Pediatric Liver Tumor) protocol-1: A report from the Japanese Study Group for Pediatric Liver Tumor. J Pediatr Surg 37:851–856.

Schlaeger C, Longerich T, Schiller C, Bewerunge P, Mehrabi A, Toedt G, Kleeff J, Ehemann V, Eils R, Lichter P, Schirmacher P, Radlwimmer B. 2008. Etiology-dependent molecular mechanisms in human hepatocarcinogenesis. Hepatology 47:511–520.

Sugawara W, Haruta M, Sasaki F, Watanabe N, Tsunematsu Y, Kikuta A, Kaneko Y. 2007. Promoter hypermethylation of the *RASSF1A* gene predicts the poor outcome of patients with hepatoblastoma. Pediatr Blood Cancer 49:240–249.

Suzuki M, Kato M, Yuyan C, Takita J, Sanada M, Nannya Y, Yamamoto G, Takahashi A, Ikeda H, Kuwano H, Ogawa S, Hayashi Y. 2008. Whole-genome profiling of chromosomal aberrations in hepatoblastoma using high-density single-nucleotide polymorphism genotyping microarrays. Cancer Sci 99:564–570.

Toledo F, Wahl GM. 2007. MDM2 and MDM4: p53 regulators as targets in anticancer therapy. Int J Biochem Cell Biol 39:1476–1482.

Traer CJ, Foster FM, Abraham SM, Fry MJ. 2006. Are class II phosphoinositide 3-kinases potential targets for anticancer therapies? Bull Cancer 93:E53–E58.

Wang J, Chin MY, Li G. 2006. The novel tumor suppressor p33ING2 enhances nucleotide excision repair via inducement of histone H4 acetylation and chromatin relaxation. Cancer Res 66:1906–1911.

Watanabe N, Haruta M, Soejima H, Fukushi D, Yokomori K, Nakadate H, Okita H, Hata JI, Fukuzawa M, Kaneko Y. 2007. Duplication of the paternal *IGF2* allele in trisomy 11 and elevated expression levels of *IGF2* mRNA in congenital mesoblastic nephroma of the cellular or mixed type. Genes Chromosomes Cancer 46:929–935.

Weber RG, Pietsch T, Von Schweinitz D, Lichter P. 2000. Characterization of genomic alterations in hepatoblastomas: A role for gains on chromosomes 8q and 20 as predictors of poor outcome. Am J Pathol 157:571–578.

Yamamoto Y, Nannya Y, Kato M, Sanada M, Levine RL, Kawamata N, Hangaishi A, Kurokawa M, Chiba S, Gilliland DG, Koeffler HP, Ogawa S. 2007. Highly sensitive method for genome wide detection of allelic composition in nonpaired, primary specimens by use of Affymetrix single-nucleotide-polymorphism genotyping microarrays. Am J Hum Genet 81:114–126.

Zielinski B, Gratias S, Toedt G, Mendrzyk F, Stange DE, Radlwimmer B, Lohmann DR, Lichter P. 2005. Detection of chromosomal imbalances in retinoblastoma by matrix-based comparative genomic hybridization. Genes Chromosomes Cancer 43:294–301.

Pediatr Surg Int (2010) 26:1025–1030
DOI 10.1007/s00383-010-2662-x

ORIGINAL ARTICLE

Surgical intervention for patent ductus venosus

Arata Kamimatsuse · Yoshiyuki Onitake · Naomi Kamei · Go Tajima · Nobuo Sakura · Taijiro Sueda · Eiso Hiyama

Published online: 27 July 2010

Abstract Patent ductus venosus (PDV) is a rare condition, which usually presents secondary to hepatic atrophy and hepatic failure. We have treated eight cases of PDV, all with hypergalactosemia and hyperbilirubinemia. Ultrasonography and three-dimensional computed tomography demonstrated communication between the portal vein and the inferior vena cava. Of the eight PDV cases, three from the older age group (ages 9, 11, and 14 years) had high-density lesions in their brain nucleus, and one case (age 19 years) had undergone prior Kasai portoenterostomy for biliary atresia. Six PDV patients underwent ligation of PDV and the remaining two cases underwent partial banding of PDV with intraoperative monitoring to maintain portal vein pressure (PVP) under 30 cm H_2O. Improvement of the intrahepatic portal vein flow was achieved by ligation or banding of PDV. Postoperatively, serum galactose and bilirubin fell to normal ranges, but portal thrombus occurred postoperatively in the first case. We subsequently administered postoperative anticoagulation in the remaining cases and experienced no major complications. These results suggest that PDV ligation and banding are effective surgical approaches for patients with PDV. Close postoperative monitoring to avoid portal thrombus is imperative in these cases.

Keywords Patent ductus venosus · Surgery · Ligation · Banding · Portal thrombosis

A. Kamimatsuse · Y. Onitake · N. Kamei · T. Sueda · E. Hiyama (✉)
Department of Pediatric Surgery,
Graduate School of Biomedical Science,
Natural Center for Basic Research and Development,
Hiroshima University, 1-2-3, Kasumi,
Minami-ku, Hiroshima 734-8551, Japan
e-mail: eiso@hiroshima-u.ac.jp

G. Tajima · N. Sakura
Department of Pediatrics, Graduate School of Biomedical Science, Natural Center for Basic Research and Development,
Hiroshima University, Hiroshima 734-8551, Japan

Introduction

Patent ductus venosus (PDV) is a rare form of congenital portosystemic shunt (PSS). Clinical symptoms and complications from PSS have not been clarified, and the natural course of this disease remains unclear [1]. Surgical treatments for PDV include ligation, banding, coiling, or stenting of the PDV, as well as liver transplantation, but there is no standard operation for symptomatic PDV [1–3]. We recently performed surgical treatment for eight cases with PDV. In this paper, we analyze these cases and show the clinical, radiological, and surgical findings in PDV cases.

Patients and methods

Eight children with a PDV underwent surgery at the Department of Pediatric Surgery in Hiroshima University Hospital during the study period of 1998–2009. All patients, except for one patient with biliary atresia, had undergone a clinical assessment and detailed biochemical investigations in the department of pediatrics. In each patient, radiological examinations included a combination of ultrasonography, computerized tomography (CT), magnetic resonance imaging, angiography, and echocardiography. We analyzed the clinical examinations, radiologic images, operative findings, including the pressure of portal

vein (PPV), and outcomes. In all patients, we analyzed their postoperative course, including hepatic hemodynamics and perioperative complications. Two patients had been followed more than 5 years before surgical consultation in the department of pediatrics, so we also investigated their change in clinical data and portal vein hemodynamics in their follow-up periods.

Results

The clinical and radiological findings for all eight patients are summarized in Tables 1 and 2. All cases except case 6 had been followed up for hypergalactosemia detected by neonatal screening. In case 6, PDV was detected by CT scan in the follow-up period for biliary atresia. This patient had undergone Kasai portoenterostomy at 3 months of age and had no evidence of portal hypertension or splenomegaly. However, progressive liver atrophy was identified at age 19 years and CT scan revealed PDV. The representative CT and angiography for cases 1 and 2 are shown in Figs. 1 and 2, respectively. As shown in Fig. 2a, CT angiography was used to reconstruct intraabdominal vessels in 3D, which was useful for evaluating PDV.

Preoperatively, hemodynamic analysis was performed in all cases, especially in cases 1, 4 and 6 (Table 2). In these three cases, the venous phase of superior mesenteric angiography revealed a PDV measuring 11, 25, and 18 mm in diameter, respectively. In these cases, portal vein and hepatic vein were atrophic when compared to the diameter of PDV (Figs. 1, 3). In the remaining five cases, CT angiography showed apparent portal and hepatic veins to have sufficient blood supply to the liver (Fig. 2). Atrophy of portal vein was defined when the diameter of the portal vein was smaller than half of the PDV diameter. In our series, the cases 1, 4, and 6 showed atrophic portal vein. In case 4, the atrophic portal vein was too small to perform selective portal venography through the vena cava (Fig. 3). Portal venography was performed during PDV occlusion using a balloon catheter introduced via the superior vena cava. We visualized the extrahepatic portal vein or the main portal vein as a fine line, <1.0 mm in diameter,

Table 1 Clinical and radiological findings

Case	Age at diagnosis	Age at surgery (y)	Symptoms	Primary disease	Serum			Radiological findings by CT and angiography			
					Galactose	Bile acid	NH_3	Liver atrophy	High-density area in brain	Portal vein atrophy	Hepatic vein atrophy
1	5 y	11	–	–	High	High	High	+	+a	+	+
2	1 m	1	–	–	High	High	High	–	–	–	–
3	1 m	9	–	Hemangioma	High	High	High	–	+a	–	–
4	4 y	14	–	–	High	High	High	+	+a	++	+
5	1 m	6	–	–	High	High	High	–	–	–	–
6	19 y	21	General tiredness	Biliary atresia	High	High	High	+	–	+	+
7	1 m	1	–	–	High	High	High	–	–	–	–
8	1 m	1	–	–	High	High	High	–	–	–	–

y year, *m* month, *a* high-density area in basal ganglia

Table 2 Operative findings of PDV cases

Case	Age at surgery (years)	PVP at laparotomy (cmH_2O)	Diameter of PDV (mm)	PVP at PDV occlusion (cmH_2O)	Liver atrophy	Regenerative nodule	Surgical procedure	PVP after surgery (cmH_2O)	Complication
1	11	6	11	19	+	+	Ligation	18	+a
2	1	9	10	17	–	–	Ligation	15	–
3	9	8	5	22	–	–	Ligation	23	+b
4	14	7	25	45	+	–	Banding	25	–
5	6	8	15	28	–	–	Ligation	28	–
6	21	6	18	40	++	–	Banding	30	–
7	1	5	6	16	–	–	Ligation	17	–
8	1	7	7	19	–	–	Ligation	16	–

y year, *PVP* portal vein pressure, *PDV* patent ductus venosus, *a* portal thrombosis, *b* hydrocele of testis

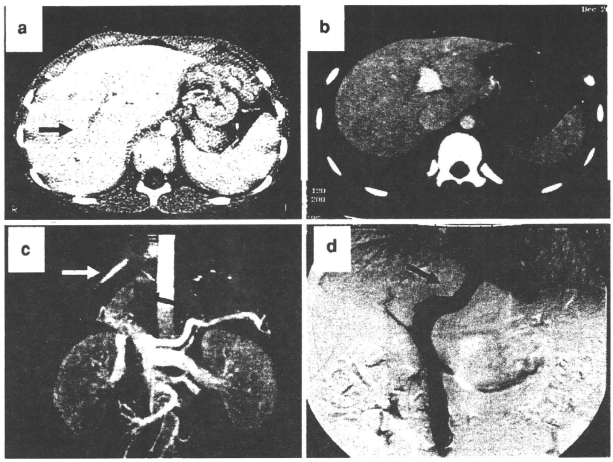

Fig. 1 Radiographic findings in case 1. Apparent intrahepatic portal vein flow (*arrow*) was detected in CT scan at age 5 years (**a**). CT angiography (**b**, **c**) and portal venography via the superior vena cava (**d**) at age 13 years revealed a large patent ductus venosus (*black arrow*) and hypoplastic portal vein. These findings suggested that hepatic atrophy had progressed in these 8 years. However, the hepatic vein (*white arrow*) was also detectable at that time

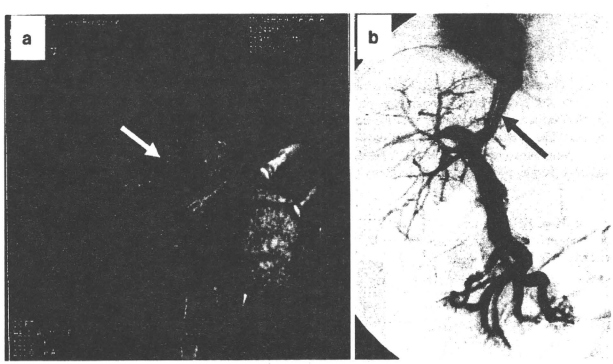

Fig. 2 CT angiography with 3D reconstruction in case 2 (1-year-old boy) with clearly visible patent ductus venosus (**a**). This is a similar grade as portal venography via the superior vena cava (**b**)

suggesting severe portal vein atrophy. Complete occlusion test of the PDV with the balloon catheter for 5 min resulted in elevation of the portal vein pressure (PVP) from 8 up to 45 cm H_2O. In cases 1 and 6, whose angiographic findings also revealed portal and hepatic vein atrophy, complete occlusion test of the PDV resulted in elevation of the PVP from 6 up to 29 cm H_2O and from 6 up to 34 cm H_2O, respectively.

Open laparotomy revealed liver atrophy in cases 1, 4, and 6 and a hepatic nodule was detected in case 1 (Fig. 4). To measure PVP, we introduced a catheter (Nipro, Osaka, Japan) from the peripheral inferior mesenteric vein to the portal vein. After manipulation of the left hepatic lobe, we detected PDV and encircled it with vessel tape. Test clamping of the PDV increased the PVP from 5–9 to 16–45 cm H_2O (Table 2). However, PVPs after occlusion were under 30 cm H_2O in cases with detectable apparent portal and hepatic veins in preoperative CT (Fig. 1). In cases 4 and 6, PVPs after temporary occlusion were >30 cm H_2O. Thus, we performed partial banding of PDV under intraoperative PVP monitoring. In fact, Teflon tape (Kono, Chiba, Japan) was banded surrounding the ductus

venosus. Banding size was controlled by the moving of the cuff using the remaining tape. It was then fixed with a 3-0 prolene suture (Fig. 3b, c) resulting in a PVP of 25–30 cm H_2O. In other cases, temporary occlusion for 20 min showed PVP of <30 cm H_2O and ligation of PDV was performed using double or triple ligation with prolene. Immediately following banding or ligation of PDV, slight intestinal congestion was observed in some cases, but no hepatic congestion or intestinal edema was noted 30 min after PDV occlusion. Biopsy was performed of normal liver in all cases and from the tumor in case 1. The abdomen was then closed in standard multilayer fashion. Microscopic examination of liver biopsy specimens did not reveal any specific findings. The tumor of case 1 was diagnosed as nodular regenerative hyperplasia.

Minor postoperative intestinal congestion was observed in all cases, which caused a hydrocele testis in case 3, but no patients had a postoperative ileus longer than 3 days after surgery. Laboratory data, including serum levels of ALT, AST, galactose, bilirubin, and ammonia, returned to normal within 7 days after surgery. However, case 1 was complicated by postoperative portal thrombosis (Fig. 4d, e). We treated this patient with heparin anticoagulation and his thrombosis resolved within 1 month after surgery. After this complication, the following seven cases underwent anticoagulation therapy for 2–3 weeks after surgery. Postoperative ultrasonography and CT scanning revealed no revascularization of ductus venosus in the cases that underwent ligation. In case 4, the shunt ratio of PDV was <10%, 1 year after surgery. Interestingly, in case 6, the PDV blood flow became undetectable 6 months after banding. The CT findings in cases 1, 4, and 6 revealed that their hepatic volume gradually enlarged after surgery.

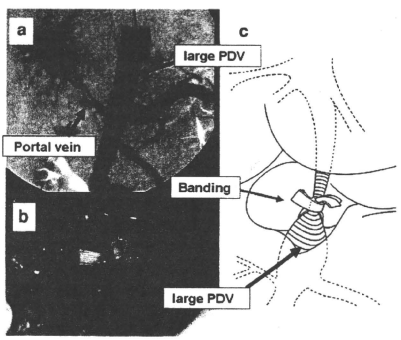

Fig. 3 Portal venography and intraoperative findings in case 4 (14-year-old girl). Portal venography via the superior vena cava (**a**) showed large patent ductus venosus and hypoplastic portal vein (*arrow*). The occlusion test for 5 min showed remarkable increase in portal vein pressure (45 cm H_2O). Therefore, banding of PDV by Teflon cuff was performed by laparotomy (**b**)

Discussion

Congenital PSS may be more common in Japan, but it is possible that these shunts are simply detected more readily because of routine newborn screening for hypergalactosemia [4, 5]. Continuous galactosemia in the absence of

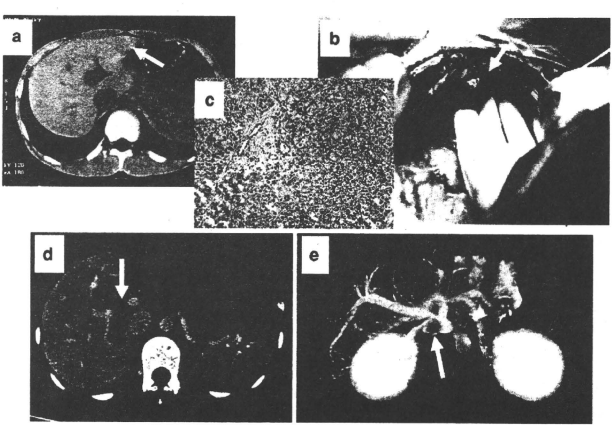

Fig. 4 Hepatic tumor and postoperative portal thrombosis in case 1. In case 1, hepatic tumor (*arrow*) was detected on CT scan (**a**) and at intraoperative findings (**b**). Histologic examination revealed a hyperplastic regenerative nodule (**c**). In this case, postoperative CT (**d**, **e**) showed intraportal thrombosis (*arrow*). This thrombosis was diminished following therapeutic anticoagulation

enzyme deficiency sometimes indicates the existence of PSS, and possibly PDV. As described by our series, PDV presents hypergalactosemia, hyperammonemia, and hyperbilirubinemia, and cases 2, 3, 5, and 7 were detected in infancy. However, before 2000, the relationship between hypergalactosemia and PDV had been unclear [6]. In cases 1, 3, and 4 born before 1999, PDV was difficult to diagnose in infancy. Thus, these cases were considered as late-phase patients with PDV.

CT angiography with 3D reconstruction is very useful for evaluating PDV. Spontaneous closure of the ductus venosus begins immediately after birth and complete functional closure usually occurs by about 17 days of age [7, 8]. Closure may be delayed temporarily in the presence of congenital heart disease, presumably as a result of elevated venous pressure, but spontaneous closure has not been reported in older patients. Of associated congenital malformations reported, cardiovascular anomalies are the most frequent [3, 4]. Biliary atresia has also been reported in several cases [9, 10]. In our series, case 6 had biliary atresia, but her PDV was not detected at the initial portoenterostomy procedure and a large one was first detected as an adolescent. These findings suggest the possibility that PDV might develop secondary to biliary atresia, resulting in atrophy of the liver.

Patients with either type of congenital PSS, including PDV, may be asymptomatic but they are prone to two specific complications: development of intrahepatic tumors and hepatic encephalopathy. PDV was previously reported to coexist with hypoplasia of the intrahepatic portal venous system [2, 11]. This is likely a consequence of PDV for two reasons. First, hypoplasia is not found in all cases; and second, the shunt can be successfully ligated without the development of portal hypertension [2, 12]. In our series, atrophy of the intrahepatic portal venous system was not found in infants. However, three older cases showed atrophy of the liver at laparotomy. In case 1, CT scan at age 5 years showed apparent portal vein flow, but CT at age 13 years showed atrophy of the intrahepatic portal vein and the liver. These findings also suggest that portal and hepatic vein flow gradually decreased in cases with PDV, resulting in apparent liver atrophy in adolescents. Thus, ligation of PDV should be performed in the early childhood period. Hepatic encephalopathy due to cerebral effects of circulating toxins, which normally undergo first pass metabolism in the liver, is another critical problem in patients with PSS. The age of onset of encephalopathy is variable and partially related to the volume and duration of the shunt [5], but hepatic encephalopathy has been diagnosed in children as young as 3 years [12]. The evidence for gradual increase in the PDV flow and progressive age-related liver atrophy may complicate hepatic encephalopathy, indicating that early surgical closure of PDV is preferable for children. In fact, cases 1 and 4 showed abnormal high-density loci on cerebral CT. Although they are currently asymptomatic, we believe these cases should be carefully followed.

Benign hepatic lesions including fatty infiltration, nodular regenerative hyperplasia, adenoma, focal nodular hyperplasia [3, 11–14, 20], and malignant liver tumors [15, 16] have been reported in PDV cases. Regression of benign tumors was reported because tumor development may be a consequence of excessive arterialization of the liver, lack of portal blood flow, and increased circulating levels of hepatic growth factors [17]. Rats with congenital portocaval shunt may also develop liver atrophy and hyperplastic nodules [18, 19]. These lesions correlate with abnormal blood circulation in the liver, and might be the cause of liver dysfunction.

For closure of PDV, potential therapeutic options include surgical ligation or radiological occlusion of the shunt. In some reports, radiologic embolization might be possible, and some patients with a shunt size of <5 mm have been successfully treated by interventional embolization [4, 21]. Occlusion of the shunt may cause portal hypertension if the native intrahepatic portal venous system becomes atrophic. Therefore, we have not attempted this procedure, because we cannot completely exclude the need to revascularize the shunt in the patient who develops intestinal congestion after occlusion or banding. Thus, surgical ligation or banding is our preferred approach if the PVP increases after test clamping of the PDV. If the patients have life-threatening complications, such as massive intestinal congestion, reoperation may be performed to release the ligation or bandings. To avoid such complications, we must assess whether PDV closure can safely accommodate the increased portal venous inflow without severe intestinal congestion from portal hypertension. CT angiography is most effective to evaluate intrahepatic portal veins and hepatic veins, as well as PDV anatomy. Portal venography during PDV occlusion with a balloon catheter introduced via the superior vena cava in cases 1 and 4 demonstrated severe atrophy of the extrahepatic and intrahepatic portal veins (Figs. 1b–d, 3a). Functionally, complete occlusion of the PDV with the balloon catheter for 5 min resulted in elevation of the portal vein pressure (PVP) from 8 up to 45 cm H_2O in case 4. Thus, in this case, we chose the banding procedure to narrow the ductus venosus instead of ligation. This radiological occlusion test is one of the useful methods for choosing surgical treatments including liver transplantation in cases with large PDV. Furthermore, surgical procedures under intraoperative PVP monitoring are safe and effective. Our series suggest that intraoperative PVP monitoring is most beneficial in the surgical decision-making process for PDV. After intraoperative testing of PDV occlusion, the patients